Nonequilibrium Blunt Body Flows in Ionized Gases

AUTHOR(S):

NISHIDA, Michio

CITATION:

NISHIDA, Michio. Nonequilibrium Blunt Body Flows in Ionized Gases. Memoirs of the Faculty of Engineering, Kyoto University 1981, 43(2): 265-286

ISSUE DATE:

1981-06-25

URL:

http://hdl.handle.net/2433/281177

Nonequilibrium Blunt Body Flows in Ionized Gases

By

Michio NISHIDA*

(Received December 27, 1980)

Abstract

The behaviors of electrons and electronically excited atoms in non-equilibrium and partially ionized blunt-body-flows are described. Formulation has been made separately in a shock layer and in a free stream, and then the free stream solution has been connected with the shock layer solution by matching the two solutions at the shock layer edge. The method of this matching is described here. The partially ionized gas is considered to be composed of neutral atoms, ions and electrons. Furthermore, the neutral atoms are divided into atoms in excited levels. Therefore, it is considered that electron energy released due to excitation, and that gained due to de-excitation, contribute to electron energy. Thus, the electron energy equation including these contributions is solved, coupled with the continuity equations of the excited atoms and the electrons. An electron temperature distribution from a free stream to a blunt body wall has been investigated for a case when the electrons are in thermal non-equilibrium with heavy particles in the free stream. In addition, the distributions of the excited atom density are discussed in the present analysis.

1. Introduction

The study of blunt body flows in ionized gas is an interesting problem which has relevance to a stagnation point electrostatic probe, and to a relaxation problem of excitation-de-excitation and ionization-recombination. Under the conditions where this problem is considered, the gas is usually partially ionized, and different non-equilibrium phenomena occur. If a blunt body is placed in an ionized supersonic flow, a detached gasdynamic shock is produced, and a thermal layer, where the electron temperature is elevated, will be formed ahead of the shock. When we consider a viscous shock layer, the thermal layer will influence the shock layer profiles of the charged particles, and the shock layer will affect the thermal layer profile of the electron temperature. Thus, an interaction between the thermal layer and shock layer will arise. Therefore, in the case of a blunt body flow in ionized gas, the thermal layer and the shock layer should be considered simultaneously.

* Department of Aeronautical Engineering

In such an ionized flow, three non-equilibrium states are observed. One is the thermal non-equilibrium, which is due to temperature differences betwene the electrons and heavy particles. A second non-equilibrium is ionizational non-equilibrium. A third non-eqiulibrium is called electronical non-equilibrium, where electronically excited levels are not populated according to the Boltzmann relation. In a laboratory experiment of such an ionized gas as an arc-heated low-density plasma, these three non-equilibrium states simultaneously exist. Therefore, we must include these non-equilibrium phenomena in the analysis of the ionized blunt body flow.

Since the work made by Talbot,[1] there has been considerable interest in the problem of the ionized blunt body flows.[2-8] However, none of these studies treated the electronical non-equilibrium. To consider the electronical non-equilibrium is identical to determining excited atom densities or population densities. The population densities contribute to a net production rate of electrons and a net electron energy transfer rate due to inelastic collisions: Ionization is considered as a transition from any excited level to an ionization limit. The local ionization rate is proportional to the population density of a level so that a distribution of the population densities is required to estimate the total ionization rate. The second contribution of the population densities is also important to estimate the electron temperature. The energies for excitation from a lower level to an upper level and for ionization are supplied from the kinetic energy of the electrons colliding with excited atoms. The energy released due to the inverse transition is gained by the electrons. Thus, the population densities play an important role for determining the electron temperature.

There are many studies concerning ionized, supersonic flows where the population densities are discussed.[9-16] However, these studies treated the problem of the population densities in a freely expanding flow, a nozzle flow, a flow field behind an ionizing shock wave and a flat plate boundary layer.

In the present study, the problem of the ionized blunt body flow is treated where there exist the above-mentioned three-typed non-equilibrium states. The analysis is made from a free stream to the surface of the blunt body. In such a flow, the electron energy equation must be analyzed separately in the free stream and the shock layer, and then the two solutions are connected at a certain position. The previously proposed method[8] was used for this procedure. The conditions here are the conditions which are established in a usual arc-heated low-density plasma.

2. Formulation in a Shock Layer

2.1 Basic Equations

The problem considered is that for a partially ionized viscous shock layer flow over a blunt body which is at floating potential. We treat the case where the Rankine-Hugoniot condition is satisfied across the shock. However, there is no such jump across the shock in the electron temperature as in the heavy-particle temperature.[20,22] In this paper, we consider the case where the electrons are in thermal non-equilibrium with heavy particles in both the viscous shock layer and the free stream. Also, this paper considers the contributions of excitation-de-excitation to electron gas as well as those of ionization-recombination. The following assumptions are introduced: (1) The gas is composed of argon atoms, ions and electrons; (2) the degree of ionization $\alpha_e \ll 1$; (3) there are no external magnetic and electric fields; (4) there is ambipolar diffusion so that $n_e = n_i$; (5) $T_a = T_i$; (6) the sheath thickness is neglected compared with the shock layer thickness; and (7) collision-free sheath is considered.

Since the degree of ionization is negligible compared with unity, the behavior of neutral particles in the ground state is not influenced by the existence of the electrons. However, the neutral particles in the excited level are affected by the electrons through electron-collisional excitation-de-excitation. In the range of electron density and population density considered here, the electron-collisional excitations from the ground level, and the de-excitations to it, do not contribute to the density of the atoms in the ground level. Therefore, it may be considered that the flow is dominated by the atoms in the ground level. Thus, over-all continuity, momentum and energy equations of the gas of interest are essentially those of the neutral particles in the ground level. Then, these equations are independently analyzed because they are not coupled with the equations of the electrons and excited atoms.

First of all, we consider the basic equations for the excited atoms. The excited atoms are assumed to have the same thermal velocity and flow velocity as the atoms in the ground level, so that the required equation for the excited atoms is a continuity equation. The energy level structure of the neutral argon atoms used here is summarized in Table 1. Under the present condition, the flow time of a gas through a shock layer is of the order of 10^{-5} s, while the relaxation time of the excited levels above level $4s$ is of an order less than 10^{-8} s. A steady state assumption may therefore be made for all the levels above level $4s$, which leads to a system of the following equations:

$$\dot{n}(j) = 0\,, \qquad j = 3, 4, 5, \cdots \tag{1}$$

Table 1. Energy Level Model of Neutral Argon.

j	Term	$g(j)$	j	Term	$g(j)$
1	$3p^6$	1	12	$7s$	12
2	$3p^5 4s$	12	13	$5f$	84
3	$4p$	36	14	$7p$	36
4	$3d$	60	15	$6d$	60
5	$5s$	12	16	$8s$	12
6	$5p$	36	17	$6f$	84
7	$4d$	60	18	$8p$	36
8	$6s$	12	19	$7d$	60
9	$4f$	84	20	$9s$	12
10	$6p$	36	21	$8d$	40
11	$5d$	60			

where $\dot{n}(j)$ is the net production rate of the j-level population density. On the other hand, the relaxation time of level $4s$ is of the order 10^{-6}–10^{-4} s, under an assumption that the radiation originating from level $4s$ is trapped so that the steady state assumption does not hold well for this level. In addition, we neglect a diffusion of excited atoms in the shock layer. This means that the excited atoms behave in the same way as the atoms in the ground level. However we must include a net production term due to transitions into the continuity equation of the excited atoms in the $4s$ level. We use the coordinate system as shown in Fig. 1., where u and v are the velocities in the x- and y-directions, respectively, and

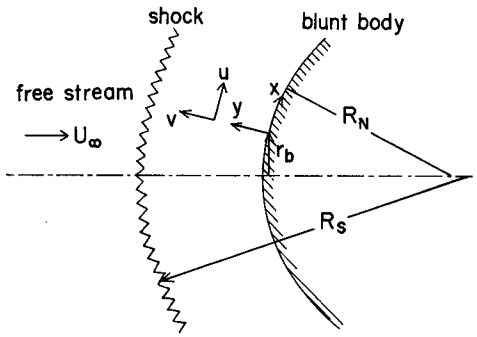

Fig. 1. Coordinates System.

U_∞ is the freestream velocity. We can write the continuity equation of the atoms in level $4s$ as follows:

$$\rho u \frac{\partial \alpha_2}{\partial x} + \rho v \frac{\partial \alpha_2}{\partial y} = m_a \dot{n} \quad (2) \tag{2}$$

with

$$\alpha_2 = n(2)/n\,, \quad \rho = m_a \sum_{j=1}^{\infty} n(j) + m_i n_i + m_e n_e\,, \quad n = \sum_{j=1}^{\infty} n(j) + n_e \simeq n(1)\,, \qquad (3)$$

where $n(2)$ is the population density of level $4s$ ($j=2$), n_i the ion density equal to the electron density n_e, $n(1)$ the density of the ground level atoms, m_a the atom mass, m_i the ion mass and m_e the electron mass.

The electron continuity and energy equations are given by[17]

$$\rho u \frac{\partial \alpha_e}{\partial x} + \rho v \frac{\partial \alpha_e}{\partial y} + \frac{\partial}{\partial y}(\rho_i V_d) = m_a \dot{n}_e, \qquad (4)$$

$$\rho u \frac{\partial}{\partial x}(\alpha_e C_p T_e) + \rho v \frac{\partial}{\partial y}(\alpha_e C_p T_e) = u \frac{\partial p_e}{\partial x} + (v + V_d)\frac{\partial p_e}{\partial y} + \frac{\partial}{\partial y}\left(\lambda_e \frac{\partial T_e}{\partial y}\right) - \frac{\partial}{\partial y}(C_p \rho_i V_d) + R + L\,, \qquad (5)$$

with

$$\alpha_e = n_e/n\,, \quad \rho_i = m_i n_e\,, \quad C_p = (5/2)k_B/m_a\,, \quad p_e = n_e k_B T_e\,. \qquad (6)$$

In Eqs. (4) and (5), V_d is the diffusion velocity, T_e the electron temperature, λ_e the thermal conductivity of the electrons, R the electron energy transfer rate due to elastic collisions, L the electron energy transfer rate due to inelastic collisions, $\dot{n}_e$ the net production rate of the electrons and k_B the Boltzmann constant.

The net production rate of atoms in level j is given by

$$\dot{n}(j) = \sum_{s=1}^{\infty} [Q(s,j) n_e n(s) - Q(j,s) n_e n(j)] + Q_R(\infty, j) n_e^2 - Q_I(j, \infty) n_e n(j) + \sum_{s=j+1}^{\infty} \beta(s,j) A(s,j) n(s) - \sum_{s=1}^{j-1} \beta(j,s) A(j,s) n(j) + \beta(\infty, j) A(\infty, j) n_e^2\,, \qquad (7)$$

where $n(j)$ is the population density of level j, $Q(s,j)$ the rate constant for an electron-collisional transition from level s to level j, $Q_I(j, \infty)$ the collisional ionization rate constant from level j, $Q_R(\infty, j)$ the collisional recombination rate constant to level j, $A(s,j)$ the Einstein A coefficient for a radiative transition from level s to level j, $A(\infty, j)$ the radiative recombination rate constant to level j and $\beta(j,s)$ the escape factor.

In the order in which they appear, the terms on the right hand side of Eq. (7) represent the following contribution to the population of the level j: electron-collisional excitation and de-excitation to the level j, electron-collisional excitation and de-excitation from the level j, collisional recombination to the level j, collisional ionization from the level j, radiative transition from an upper level to the

level j, radiative transition from the level j to a lower level, and radiative recombination to the level j. Atom-collisional transitions are insignificant compared with electron-collisional transitions in the present condition. In addition, it is assumed that radiation terminated in any excited level is completely optically thin, which leads to the escape factor being unity. On the other hand, for the resonance radiation the escape factor is applied.

Now, we express the net production rate of the electrons in terms of population densities and rate constants of collisional ionization and recombination. The collisional ionization rate from level j is expressed as $n_e n(j) Q_I(j, \infty)$. The rate of inverse process is obtained by substituting for $n(j)$ the equilibrium value $n_{eq}(j)$ from the Saha equation, because the two rates must be equal at equilibrium. The net rate of the electron production will be therefore obtained by summing $Q_I(j, \infty) n_e n(j) - Q_I(j, \infty) n_e n_{eq}(j)$ over j from $j=1$ to $j=\infty$ where $n_{eq}(j)$ is taken as being in equilibrium with free electrons. The equilibrium population density $n_{eq}(j)$ is given by the following Saha equation:

$$n_{eq}(j) = n_e^2 \frac{g(j)}{2Z_i} \left(\frac{h^2}{2\pi m_e k_B T_e} \right)^{3/2} \exp\left(\frac{E_I - E_j}{k_B T_e} \right), \tag{8}$$

where $g(j)$ is the statistical weight of the level j, Z_i the partition function of ions expressed as $4+2\exp(-2062/T_e)$, h the Planck's constant, E_I the ionization energy from the ground level, E_j the excitation energy of the level j from the ground level. Thus, $\dot{n}_e$ is expressed as

$$\dot{n}_e = n_e \sum_{j=1}^{\infty} [Q_I(j, \infty) \{n(j) - n_{eq}(j)\}] . \tag{9}$$

The electron energy transfer rate due to the inelastic collision, L, includes those due to the collisional transitions between the bound levels, due to the collisional ionization-recombination and also to the radiative recombination. It is written as

$$\begin{aligned} L = & - \sum_{k=2}^{\infty} \sum_{j=1}^{k-1} (E_k - E_j)[Q(j, k) n_e n(j) - Q(k, j) n_e n(k)] \\ & - n_e \sum_{j=1}^{\infty} (E_I - E_j)[n(j) - n_{eq}(j)] Q_I(j, \infty) \\ & - \frac{3}{2} k_B T_e n_e^2 \sum_{j=1}^{\infty} \beta(\infty, j) A(\infty, j) , \end{aligned} \tag{10}$$

for $k > j$. By multiplying Eq. (7) by $(E_I - E_j)$, summing up all j, and then using the resultant equation in Eq. (10), we obtain

$$L = \sum_{j=1}^{\infty} (E_I - E_j) \dot{n}(j) + L_{rad} , \tag{11}$$

where

$$L_{rad} = -\sum_{k=2}^{\infty}\sum_{j=1}^{k-1}\beta(k,j)A(k,j)n(k)(E_k-E_j) - \sum_{k=1}^{\infty}\beta(\infty,k)A(\infty,k)n_e^2[E_I-E_k+(3/2)k_BT_e]\,. \tag{12}$$

Since we have assumed the steady state population $\dot{n}(j)=0$ for $j\geqq 3$, Eq. (11) is rewritten as

$$L = \dot{n}(1)E_I+\dot{n}(2)(E_I-E_2)+L_{rad}\,. \tag{13}$$

The electron energy transfer rate due to the elastic collisions, R, is expressed as

$$R = 2n_em_e\sum_j\frac{\bar{\nu}_{ej}}{m_j}\left[\frac{3}{2}k_B(T_j-T_e)\right], \tag{14}$$

where $\bar{\nu}_{ej}$ represents the collision frequency for the electron-j-species encounters, m_j the mass of the j-species and T_j the temperature of the j-species. Using the Coulomb cross section for the electron-ion encountres, the average electron-ion collision frequency is of the form[18]

$$\bar{\nu}_{ei} = \frac{8}{3}\left(\frac{\pi}{m_e}\right)^{1/2}\frac{n_ee^4}{(2k_BT_e)^{3/2}}\ln\left(\frac{9k_B^3T_e^3}{4\pi n_ee^6}\right), \tag{15}$$

where e is the electronic charge. By assuming that an effective cross section for the electron-atom encounters is constant, the average collision frequency is expressed as[19]

$$\bar{\nu}_{ea} = n_a(8k_BT_em_e)^{1/2}\sigma_{ea}\,. \tag{16}$$

For the argon atom, σ_{ea} is approximately expressed as[17]

$$\begin{aligned}\sigma_{ea} &= (0.39-0.551\times10^{-4}T_e+0.595\times10^{-8}T_e^2)\times10^{-20}\,m^2 \quad \text{for} \quad T_e<10^4\,\text{K}\,,\\ \sigma_{ea} &= (-0.35+0.775\times10^{-4}T_e)\times10^{-20}\,m^2 \quad \text{for} \quad T_e\geq10^4\,\text{K}\,.\end{aligned} \tag{17}$$

The thermal conductivity of species j of a gas mixture is given by[20]

$$\lambda_j = \frac{75k_B}{16}\frac{n_jk_BT_j}{m_j}\left[\sum_k n_k\sigma_{jk}\left(\frac{8k_BT_j}{\pi m_j}+\frac{8k_BT_k}{\pi m_k}\right)\frac{2m_{jk}}{m_j}\right]^{-1}, \tag{18}$$

where $m_{jk}=m_jm_k/(m_j+m_k)$ and n_j is the density of species j. When $T_e/m_e\gg T_i/m_i$, the relation $\sigma_{ei}=\sigma_{ee}$ holds well. Using the Coulomb cross section for σ_{ee}, we have

$$\lambda_e = \frac{75k_B}{64\sqrt{2}}\left(\frac{\pi k_BT_e}{m_e}\right)^{1/2}\frac{n_e}{n_a\sigma_{ea}+(1+\sqrt{2})n_e\sigma_{ee}}\,. \tag{19}$$

The ambipolar diffusion velocity is given by

$$V_d = -\frac{D_a}{\alpha_e}\left[\nabla\alpha_e + \frac{\alpha_e(1-\alpha_e)}{1+\Omega}\nabla\Omega\right], \quad \text{(See Appendix)} \tag{20}$$

where $\Omega = T_e/T_a$ and D_a is the ambipolar diffusion coefficient defined by

$$D_a = \frac{\bar{\mu}_e\bar{\mu}_i}{\bar{\mu}_e+\bar{\mu}_i}\frac{k_B T_a}{e}\frac{1+\Omega}{1+\alpha_e\Omega}, \tag{21}$$

in which $\bar{\mu}_e$ and $\bar{\mu}_i$ are the mobilities of the electrons and ions, respectively. Using the relation $\bar{\mu}_e \gg \bar{\mu}_i$ and $\bar{\mu}_i \simeq e/m_i\bar{\nu}_{ia}$, Eq. (21) becomes

$$D_a = \frac{k_B T_a}{m_i\bar{\nu}_{ia}}\frac{1+\Omega}{1+\alpha_e\Omega}, \tag{22}$$

with

$$\bar{\nu}_{ia} = n_a(8k_B T_i/\pi m_i)^{1/2}\sigma_{ia}. \tag{23}$$

2.2 Boundary Conditions

If a body which is electrically insulated or to which the electric field is not applied, is placed in the ionized gas, it will be at floating potential, and ion sheath will be produced near the wall of the body. In this case, the net currents normal to the wall vanish. The condition of no normal net currents, and the continuity conditions at the sheath edge for fluxes of electron energy and ion mass, lead to the following boundary conditions at the wall:[8]

$$(\partial\alpha_e/\partial y)_w = D_{aw}^{-1}(k_B T_{ew}/m_a)^{1/2}\alpha_{ew}, \tag{24}$$

$$(\partial T_e/\partial y)_w = -1/2[1+\ln(2\pi)+\ln\varepsilon]n_{ew}(k_B T_{ew})^{3/2}/\lambda_{ew}m_a^{1/2}, \tag{25}$$

where $\varepsilon = m_e/m_a$, and the subscript w denotes the wall condition. The boundary conditions at the edge of the shock layer for α_2 and α_e are

$$\begin{aligned} \alpha_2(y_s) &= \alpha_{2s} = \alpha_{2\infty}, \\ \alpha_e(y_s) &= \alpha_{es} = \alpha_{e\infty}, \end{aligned} \tag{26}$$

where the subscripts s and ∞ denote the edge of the shock layer and the free stream, respectively. These boundary conditions imply frozen ionization-recombination and excitation-de-excitation across the shock. The boundary condition for the electron temperature at the edge of the shock layer is $T_e(y_s) = T_{es}$. The quantity T_{es} must be determined by matching the shock layer solution for T_e with the free stream solution at the edge of the shock layer. The method of matching will be described later.

2.3 Coordinate Transformation

In order to obtain a similar solution near the stagnation stream line, the fol-

lowing transformation of coordinates is employed:

$$\xi(x) = \int_0^x (\rho\mu)_s u_s r_b^{2j} dx\,, \quad \eta(x,y) = u_s r_b^j/(2\xi)^{1/2} \int_0^y \rho dy\,, \tag{27}$$

where $j=0$ and $j=1$ represent a two-dimensional flow and an axisymetric flow, respectively, and μ is the viscosity. In addition, the following dimensionless quantities are introduced:

$$\begin{aligned} V &= \frac{2\xi}{(\rho\mu)_s u_s r_b^{2j}}\left[f'\frac{\partial\eta}{\partial x} + \frac{\rho v r_b^j}{(2\xi)^{1/2}}\right], \\ f' &= u/u_s, \qquad \theta = T_a/T_{as}\,, \\ \Theta &= T_e/T_{a\infty}\,, \quad z = \alpha_e/\alpha_{es}\,, \quad \bar{\Omega} = \Theta/\theta\,. \end{aligned} \tag{28}$$

Using Eqs. (27) and (28), Eqs. (2), (4) and (5), near the stangation stream line, are transformed to:

$$\frac{d\alpha_2}{d\eta} = \frac{\tau_u}{n_s}\frac{\theta}{V}\dot{n}(2)\,, \tag{29}$$

$$\frac{d}{d\eta}\left(\frac{l}{Sc_a}\frac{dz}{d\eta}\right) + \frac{d}{d\eta}\left[\frac{l}{Sc_a}\frac{\tau(1-\alpha_{es}z)z}{1+\bar{\Omega}}\frac{d\bar{\Omega}}{d\eta}\right] - V\frac{dz}{d\eta} = -\tau_u\frac{m_a\dot{n}_e}{\rho\alpha_{es}}\,, \tag{30}$$

$$\begin{aligned} &\frac{d}{d\eta}\left(\frac{l}{Pr_e}\frac{d\Theta}{d\eta}\right) + \alpha_{es}\frac{d}{d\eta}\left[\Theta\left\{\frac{l}{Sc_a}\frac{d}{d\eta} + \frac{l}{Sc_a}\frac{\tau z(1-\alpha_{es}z)}{1+\tau\bar{\Omega}}\frac{d\bar{\Omega}}{d\eta}\right\}\right] \\ &\quad - \alpha_{es}V\frac{d}{d\eta}(z\Theta) + \frac{2}{5}\frac{\alpha_{es}}{\Psi}\left[V - \frac{l}{Sc_a}\frac{1}{z}\frac{dz}{d\eta} - \frac{l}{Sc_a}\frac{\tau(1-\alpha_{es}z)}{1+\tau\bar{\Omega}}\frac{d\bar{\Omega}}{d\eta}\right]\frac{d}{d\eta}(z\Theta\Psi) \\ &\quad + \tau_u\frac{R+L}{C_p T_{a\infty}\rho} = 0\,, \end{aligned} \tag{31}$$

where

$$\begin{aligned} &\tau_u = 2\xi/(\rho\mu)_s u_s^2 r_b^{2j}\,, \quad \Psi = n_e/n_{es} = z/\theta\,, \quad l = \rho\mu/(\rho\mu)_e\,, \\ &Pr_s = \mu C_p/\lambda_e\,, \quad Sc_a = \mu/\rho D_a\,, \quad \tau = T_{a\infty}/T_{as} \end{aligned} \tag{32}$$

Using the relation $\mu=(5\pi/32)(8k_BT_a/\pi m_a)/\sigma_{aa}$, and Eqs. (22) and (23), the ambipolar Schmidt number Sc_a is written as

$$Sc_a = \frac{5}{4}\frac{\sigma_{ia}}{\sigma_{aa}}\frac{(1-\alpha_e)(1+\alpha_e\tau\bar{\Omega})}{1+\tau\bar{\Omega}}\,, \tag{33}$$

where

$$\sigma_{aa} = 1.70\times10^{-18}T_a^{-1/4} \quad (\mathrm{m}^2) \tag{34}$$

Near the stagnation stream line $r_b=x$ and $u_s=u_{1s}x$, where $u_{1s}=U_\infty/R_N$, so that τ_u is rewritten as

$$\tau_u = 1/[(1+j)u_{1x}]\,. \tag{35}$$

The boundary conditions (24) and (25) are transformed to

$$\left(\frac{dz}{d\eta}\right)_w = \left[\frac{1}{1+j}\frac{(\rho\mu)_s}{u_{1s}}\right]^{1/2} \frac{Sc_{aw}}{\mu_w}\left(\frac{kT_{a\infty}}{m_a}\right)^{1/2} \Theta_w^{1/2} z_w - \frac{\tau z_w(1-\alpha_{es}z_w)}{1+\tau\Theta_w/\theta_w}\left[\frac{1}{\theta_w}\left(\frac{d\Theta}{d\eta}\right)_w - \frac{\Theta_w}{\theta_w^2}\left(\frac{d\theta}{d\eta}\right)_w\right], \tag{36}$$

$$\left(\frac{d\Theta}{d\eta}\right)_w = -\frac{1}{1+j}\frac{(\rho\mu)_s}{u_{1s}}\frac{1+\ln(2\pi\varepsilon)}{2}\frac{k_B^{3/2}\alpha_{es}T_{a\infty}^{1/2}}{m_a^{3/2}}\frac{z_w\Theta_w^{3/2}}{\lambda_{ew}}. \tag{37}$$

2.4 Over-all Basic Equations

The equations of continuity, momentum and energy given by Blottner[21] are used as the basic over-all equations. Near the stagnation stream line, these equations are written as follows:

Continuity:

$$dV/d\eta + f' = 0, \tag{38}$$

Momentum:

$$\frac{d}{d\eta}\left(l\frac{df'}{d\eta} - V\frac{df'}{d\eta} - \bar{\beta}\left(\frac{\theta}{\bar{e}} + f'^2\right)\right) = 0, \tag{39}$$

Energy:

$$\frac{d}{d\eta}\left(\frac{l}{Pr}\frac{dg}{d\eta}\right) - V\frac{dg}{d\eta} = 0, \tag{40}$$

with

$$g = H/H_s, \quad Pr = \mu C_p/\lambda, \quad \bar{\beta} = (2\xi/u_s)(du_s/d\xi), \quad \bar{e} = \rho_s\mu_s(du_s/dx)/(dp/dx), \tag{41}$$

where H is the total enthalpy, p the pressure and λ the thermal conductivity expressed as $\lambda = \lambda_a + \lambda_i + \lambda_e \simeq \lambda_a$. According to Blottner,[21] $\bar{e}$ obtained from the normal momentum equation is written as

$$\bar{e} = -\frac{1}{2\omega}\left[\frac{1-\omega}{\{1-\omega(1-1/s)\}^2} + \{(1+j)Re_s\omega[s(1-\omega)+\omega\}^{-1/2}\int_\eta^{\eta_s} f'^2 d\eta\right]^{-1}, \tag{42}$$

with

$$s = (R_N/R_s)[1+(y_s/R_N)], \quad Re_s = \rho_\infty U_\infty R_N/\mu_s, \quad \omega = \rho_\infty/\rho_s. \tag{43}$$

The boundary conditions for V, f' and g are

$$V(0) = 0, \quad f'(0) = 0, \quad g(0) = g_w, \quad V(\eta_s) = -\{\omega Re_s/2[s(1-\omega)+\omega\}]^{1/2}, \quad f'(\eta_s) = 1, \quad g(\eta_s) = 1. \tag{44}$$

Since $y_s \ll R_N$, it follows that $s \simeq 1$. Using this relation and an approximation $R_s \simeq R_N$, Eq. (42) is rewritten in the form

$$\bar{e} = -\frac{1}{2\omega}\left[1-\omega+\frac{1}{(2Re_s\omega)^{1/2}}\int_{\eta}^{\eta_s} f'^2 d\eta\right]^{-1}. \tag{45}$$

Furthermore $V(\eta_s)$ is expressed as $-(\omega Re_s/2)^{1/2}$.

3. Formulation in a Free Stream

In the free stream condition considered here, the relaxation time of all the levels above $4s$ ($j=3$) is less than the flow time of the gas, so that the steady state populations can be taken for such levels. On the other hand, both the relaxation time of level $4s$ ($j=2$) and that of ionization-recombination are larger than the flow time. Hence we can assume that $n(2)=$const and $n_e=$const in the free stream. Since the electron temperature is generally higher than the heavy particle temperature, the electron temperature decreases toward the shock due to a thermal relaxation, but near the shock it increases due to a thermal layer effect. This was analyzed by Grewal and Talbot[22] for the normal shock in partially ionized argon. The thermal layer of the electrons is produced by large thermal conductivity of the electrons. Then, it is necessary to solve the electron energy equation including a thermal conduction term to determine an electron temperature profile in the free stream. If we consider the problem near the stagnation stream line, the detached bow shock may be regarded as a normal shock, as shown in Fig. 2, where the flow is taken as a one-dimensional flow. The one-dimensional electron energy equation is written as

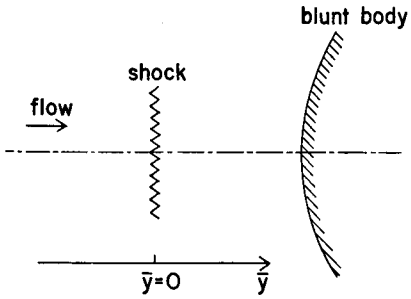

Fig. 2. Flow Model near Stagnation Streamline.

$$\frac{3}{2}\bar{u}\frac{d}{d\bar{y}}(n_e k_B T_e) = -\frac{5}{2}n_e k_B T_e\frac{d\bar{u}}{d\bar{y}}+\frac{d}{d\bar{y}}\left(\lambda_e\frac{dT_e}{d\bar{y}}\right)+R+L, \tag{46}$$

where $\bar{u}$ is the velocity in the $\bar{y}$-direction. The relation between $\bar{y}$ and y is $\bar{y}+y=y_s$. The terms R and L in Eq. (46) have the same expressions as given in Eqs. (13) and (14), respectively. The following dimensionless quantities are introduced:

$$\begin{aligned}&\Theta = T_e/T_{a\infty}, \quad \Phi = T_a/T_{a\infty}, \quad \Xi = n_e/n_{e\infty} = U_\infty/\bar{u},\\ &\lambda_e/\lambda_{er} = (\Theta/\tilde{\tau})^{5/2}, \quad \tilde{\tau} = T_{er}/T_{a\infty},\end{aligned} \tag{47}$$

where the subscripts r and ∞ denote the condition at the reference point ahead of the shock, and the condition in the free stream, respectively. In the present analysis, the point, where a decrease in the electron temperature due to the relaxation effect counterbalances an increase due to the thermal conduction, is taken as the reference point. Using Eq. (47) and the coordinate transformation $\zeta=(3/2)\times(\tilde{\tau}^{5/2}n_{e\infty}U_\infty k_B/\lambda_{er})\bar{y}$, Eq. (46) is transformed to

$$\frac{d}{d\zeta}\left(\Theta^{5/2}\frac{d\Theta}{d\zeta}\right)-\frac{d\Theta}{d\zeta}+\frac{2}{3}\frac{\Theta}{\Xi}\frac{d\Xi}{d\zeta}+\frac{R+L}{a}=0\,, \tag{48}$$

with

$$a=(9/4)(k_B^2\tilde{\tau}^{5/2}n_{e\infty}^2U_\infty^2T_{a\infty}/\lambda_{er})\,. \tag{49}$$

The parameter a denotes the characteristic electron energy transfre rate due to thermal conduction. In the upstream of the shock, $\Xi=$const so that we have

$$\frac{d}{\zeta d}\left(\Theta^{5/2}\frac{d\Theta}{d\zeta}\right)-\frac{d\Theta}{d\zeta}+\frac{R+L}{a}=0\,. \tag{50}$$

The boundary conditions are

$$\Theta=\tilde{\tau}\,,\quad d\Theta/d\zeta=0\qquad\text{at}\quad\zeta=\zeta_r\,. \tag{51}$$

The reference point ζ_r is unknown. It will be determined by matching the electron temperature profile in the shock layer with that in the free stream at the shock. The method of matching will be described in the following section.

4. Matching of Shock Layer Solution of Electron Temperature with Free Stream Solution

The electron temperature profile across the shock layer must be matched with that in the free stream. The point immediately behind the shock is selected as a matching point. Integrating Eq. (48) from $\zeta=-0$ to $\zeta=+0$, we have

$$\left[\Theta^{5/2}\frac{d\Theta}{d\zeta}\right]_{+0}-\left[\Theta^{5/2}\frac{d\Theta}{d\zeta}\right]_{-0}-\Theta_{+0}+\Theta_{-0}+\frac{2}{3}\int_{-0}^{+0}\Theta\frac{d}{d\zeta}(\ln\Xi)d\zeta+\frac{1}{a}\int_{-0}^{+0}(R+L)d\zeta=0\,. \tag{52}$$

The electron temperature does not vary across the shock[20,22] so that $\Theta_{+0}=\Theta_{-0}=\Theta_0=$ const. Introducing a new variable $Y=\Theta^{5/2}d\Theta/d\zeta$, Eq. (52) is rewritten as

$$Y_{+0}-Y_{-0}+(2/3)\Theta_0\ln\left[1+3(M_\infty^2-1)/(M_\infty^2+3)\right]=0\,, \tag{53}$$

where M_∞ is the free stream Mach number, and the subscripts $+0$ and -0 denote the conditions immediately behind and ahead of the shock, respectively. In Eq. (53), we have considered that the electron density across the shock obeys the

Rankine-Hugoniot relation. Equation (53) represents the discontinuity of the electron temperature gradient across the shock.

In Fig. 3, the method of matching is shown for $\tilde{\tau}=5$. The curve Γ_1 is obtained by integrating Eq. (50) with the boundary condition (51). The result has

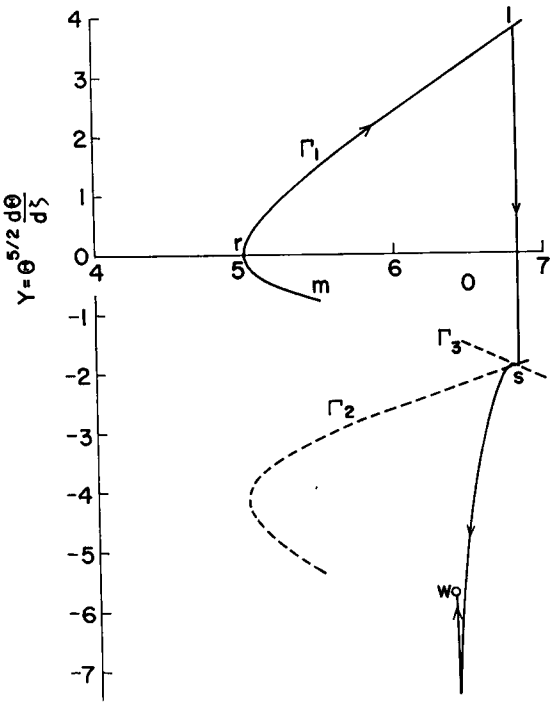

Fig. 3. Matching of Frees Stream Solution of Electron Temperature with Shcok-Layer Solution.

been plotted on the $\Theta-Y$ plane. In this stage, the reference point ζ_r can be arbitrarily selected. The position r represents the reference point, which is chosen as the point where the decrease in the electron temperature due to the relaxation effect counterbalances its increase due to the thermal conduction. The positive part of the curve Γ_1 shows the condition in the downstream of the reference point, and the negative part represents the condition in its upstream.

The curve Γ_2 expresses the locus of Y_{+0} obtained from Eq. (53). Then, the curve Γ_2 shows the condition immediately behind the shock which is obtained from the free stream solution. The curve Γ_3 can be obtained as follows: One must try to integrate Eq. (31), coupled with Eqs. (1), (29) and (30), for the different values of Θ_w, starting at the wall, and so one can obtain the values of Θ and $d\Theta/d\eta$ at $\eta=\eta_s$. Then, one can determine the value of Y_s. By plotting the values of Θ_s

and Y_s on the $\Theta-Y$ plane, the curve Γ_3 is obtained. Therefore, the curve Γ_3 shows the locus of Y_s for the different vlaues of Θ_w. Thus, the intersection of Γ_2 and Γ_3 represents the condition at the edge of the shock layer. Then, the curve s—w is the valid solution across the shock layer, and the position 1 corresponds to the condition immediately ahead of the shock. Thus, the curve m—r—1—s—w expresses the electron temperature solution from the free stream to the wall. From this result, the value of the reference point ζ_r can be determined.

5. Transition Rate Constants

Several excitation rate constants for neutral argon, calculated from analytical cross-section formulae by assuming a Maxwellian electron velocity distribution, have been proposed. These involved those of Thomson[23] and Gryzinski[24] (classical), Seaton[25] and Sobleman[26] (quantum-mechanical) and Drawin[27] (semi-empirical). The first three constants are for optically-allowed transitions while the Sobelman and Drawin constants are both for optically-allowed and parity-forbidden transitions. The Sobelman expressions for optically-allowed and parity-forbidden transitions include two parameters correspondnig to each excitation, and these parameters are not complete for a neutral-argon level model such as that used here. For the present work, Drawin's expression has been employed which, for optically-allowed transitions, is

$$Q(j,k) = 4\pi a_0^2 K(j,k) f_{j,k} \bar{v} \left(\frac{Ry}{k_B T_e}\right)^2 \frac{\exp(-u_{j,k})}{u_{j,k}(u_{j,k}+1)} \times \left\{\frac{1}{20+u_{j,k}} + \ln\left[1.25\delta_{j,k}\left(1+\frac{1}{u_{j,k}}\right)\right]\right\}, \tag{54}$$

and, for parity-forbidden transitions, is

$$Q(j,k) = 4\pi a_0^2 K(j,k) \bar{v} u_{j,k} \left[\frac{\exp(-u_{j,k})}{u_{j,k}} - \int_{u_{j,k}}^{\infty} \frac{\exp(-x)}{x}\, dx\right], \tag{55}$$

where a_0 is the first Bohr radius, Ry the Rydberg constant, $\bar{v}$ the mean electron velocity expressed as $(8k_B T_e/\pi m_e)^{1/2}$, $f_{j,k}$ the absorption oscillator strength, $K(j,k)$ a parameter introduced to achieve numerical agreement with the experiment, $\delta_{j,k}$ the shape parameter, and $u_{j,k}=|E_j-E_k|/k_B T_e$.

The optically-allowed and parity-forbidden transitions are separately treated in the present work. Spin-forbidden transitions are negligible, and the shape parameter, $\delta_{j,k}$, is assumed to be unity for all transitions except the $3p$–$4s$. From Katsonis' fitting[28] of Drawin's excitation rate constant to experimental data, $K(1.2)=0.8908$ and $\delta_{1,2}=0.8$ are obtained.

For ionizations, Drawin's expression has been used. It is written as

$$Q_I(j,\infty) = 4\pi a_0^2 v\left(\frac{Ry}{k_B T_e}\right)^2 \frac{\exp(-u_{j,\infty})}{u_{j,\infty}(u_{j,\infty}+1)} \times\left\{\frac{1}{20+u_{j,\infty}}+\ln\left[1.25\left(1+\frac{1}{u_{j,\infty}}\right)\right]\right\}, \tag{56}$$

where $u_{j,\infty}=(E_I-E_j)/k_B T_e$.

The radiative transition probabilities (Einstein A coefficient) between bound excited levels have been calculated from the direct integration of the wave function given by Bates and Damgaard.[29] As a first approximation, radiations terminated in any level except for the ground level are taken to be optically thin, which leads to the radiative-escape factor being unity. On the other hand, absorption coefficients for radiations terminated in the ground level are large enough to assume almost an immediate capture of all emissions. It is therefore appropriate to take the radiative-escape factor to be zero.

6. Calculated Results and Discussions

The conditions in the present analysis are as follows:

$M_\infty = 4.5$, $R_N = 4\times10^{-2}$ m, $T_{a\infty}$ =500 K, $n_{a\infty} = 10^{21}$ m^{-3},
$n_{e\infty} = n_{i\infty} = 5\times10^{18}$ m^{-3}, $Re_s = 28.9$, $T_w = 300$ K.

First of all, the over-all equations (38), (39) and (41), which are not coupled with the equations of the electrons and excited atoms, have been solved using an iteration method. The results are shown in Fig. 4. Thus, the obtained distributions

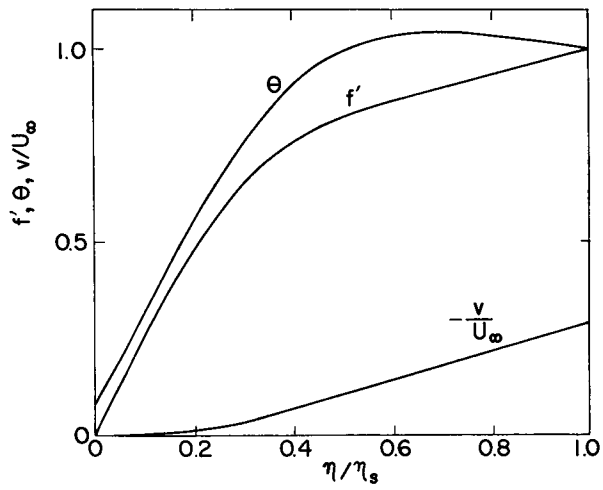

Fig. 4. Distributions of θ, f' and $-v/U_\infty$ in the Shock Layer.

of V, θ and $d\theta/d\eta$ are employed in Eqs. (29)–(31).

By taking $l=Sc_a=1$ and $\dot{n}_e=0$ in Eq. (30), a frozen solution of z can be easily obtained. Using this solution in Eq. (31), an electron temperature solution is obtained. These solutions of z and Θ are used in Eq. (29). The next step is to solve Eq. (30) by using the solutions of Θ and α_2. Thus, the calculations are made by means of an interation scheme. At each step population densities of excited levels are required so that a system of 18 linear equations (1) are coupled with Eqs. (29), (30) or (31).

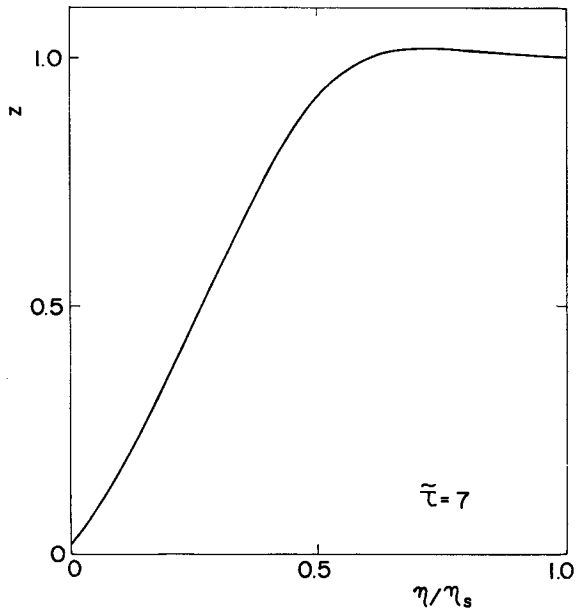

Fig. 5. Distribution of z in the Shock Layer.

In Fig. 5 is shown the distribution of z in the shock layer for $\tilde{\tau}=7$. The value of $\tilde{\tau}$ is taken at the reference point where the electron temperature gradient vanishes in the free stream.

Figure 6 illustrates the electron-temperature distributions from the position of $y/y_s=10$ to the blunt-body wall ($y/y_s=0$), for the three cases of $\tilde{\tau}=3$, 5 and 7. In the upstream region, the electron temperature decreases in order to accomplish a temperature equilibrium state between the electrons and heavy particles. The increase in the electron temperature ahead of the shock is due to electron-thermal conduction. Behind the shock, say, in the shock layer, it decreases toward the wall. It is clear that the temperature variation becomes larger with the decrease in the value of $\tilde{\tau}$. The position, where the increase in the electron temperature

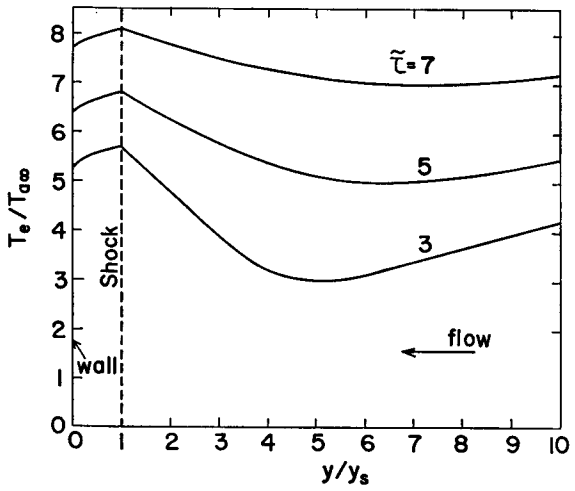

Fig. 6. Electron Temperature Distributions from Free Stream to Wall.

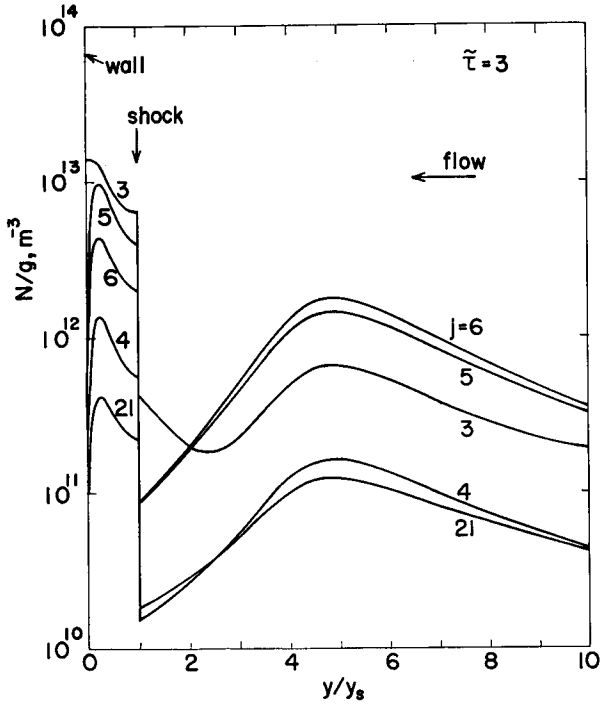

Fig. 7. Population Density Distributions from Free Stream to Wall for $\tau=3$.

due to the thermal conduction counterbalances the decrease due to the temperature equilibration, approaches the shock with the decrease in the value of $\tilde{\tau}$.

In Figs. 7 to 9, the population densities of the excited levels are illustrated for $\tilde{\tau}=3$, 5 and 7, respectively. In Fig. 7, the population densities increase in the region from $y/y_s=10$ to $y/y_s=5$. This will be due to the decrease in the electron temperature. When the electron temperature decreases, the population densities of the upper levels which are in equilibrium with free electrons, increase. This increase propagates down to the lower levels and consequently, the population densities of the lower levels increase. Between $y/y_s=1$ and 5, the population densities decrease toward the shock, corresponding to the increase in the electron temperature. The population density of level $j=3$ increases near the shock. This is because the population density of this level increases due to excitations from level $j=2$ to level $j=3$. In the case of $\tilde{\tau}=5$, the population density of level $j=4$ is also influenced by the increase in the population density of level $j=3$. In the case of $\tilde{\tau}=7$, the increase in the population density of level $j=4$ is large, and the population density of level $j=5$ also shows an increase near the shock.

Grewal and Talbot[22] mentioned a dark space ahead of a normal shock in

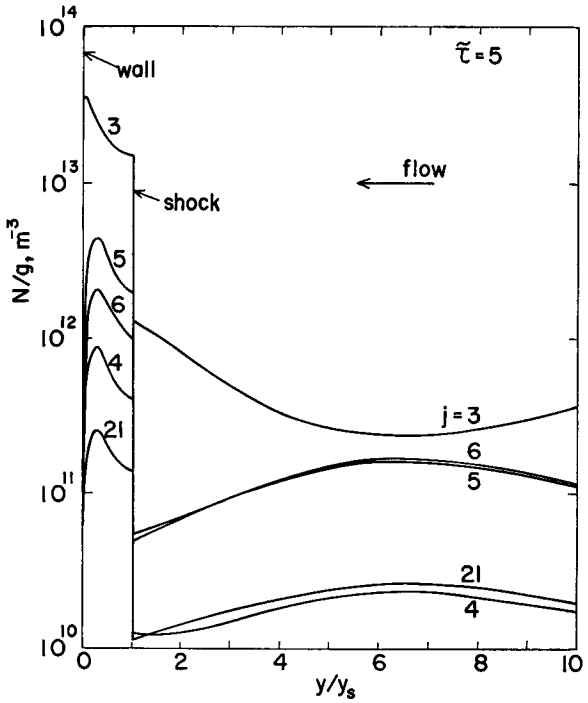

Fig. 8. Population Density Distributions from Free Stream to Wall for $\tilde{\tau}=5$.

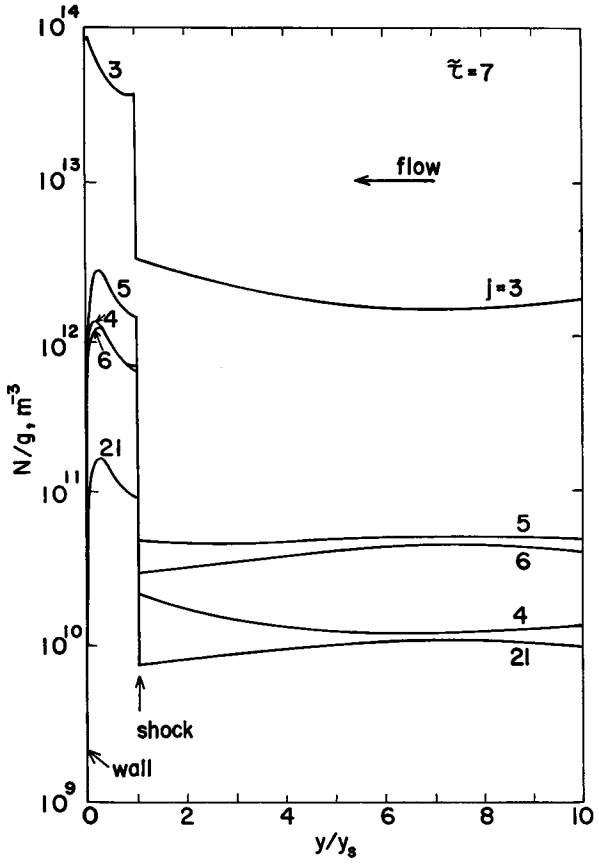

Fig. 9. Population Density Distributions from Free Stream to Wall for $\bar{\tau}=7$.

ionized gas, which is a region where the self-liuminosity of the plasma flow is reduced. They explained as follows: The dark space is due to the reduced recombination radiation which is produced by the reduction in the recombination rate. The region of the elevated electron temperature ahead of the neutral shock is a region of reduced recombination rate. Their explanation is not complete, because the reduction in the radiation intensity is associated with the reduction in atom densities in excited levels, so that a detailed study of population densities is required to reveal the dark space. In the present study, the region of the reduction in the population densities ahead of the shock exists, which corresponds to the region of the elevated electron temperature. This region of the reduced population density will be an explanation for the dark space. When the electron temperature is high, the dark space for the radiations originated from lower levels does not appear, as shown in Figs. 7 to 9.

7. Concluding Remarks

The principal conclusions which may be drawn from this investigation are summarized as follows:

1) Even when the effects of the electron energy exchange due to inelastic collisions, namely ionization-recombination and excitation-de-excitation, are included in the electron energy equation, in the free stream the electron temperature decreases toward the shock and then increases due to the effect of electron-thermal conduction.

2) The population densities are reduced ahead of the shock, corresponding to the elevation of the electron temperature. The region of the reduced population density may be explained as the so called dark space where the radiation intensity is reduced.

3) With the increase in the electron temperature at the reference point in the free stream, the reduction in the population density ahead of the shock becomes smaller. The population density of level $j=3$ is elevated there, rather than reduced, in the case $\tilde{\tau}=3$. However, in the case of $\tilde{\tau}=7$, the population density of level $j=5$ also shows an elevation ahead of the shock. Such an elevation in the population density results from the excitation from level $j=2$, so that it may be mentioned that the dark space is influenced by the population density of level $j=2$.

References

1) L. Talbot, Phys. Fluids **3**, 289 (1960).
2) P.M. Chung, Phys. Fluids **7**, 110 (1964).
3) P.M. Chung, AIAA J. **3**, 817 (1965).
4) C.H. Su, AIAA J. **3**, 842 (1965).
5) G.A. Shelton, Jr., K.T. Touryan, and D.H. Johnson, Phys. Fluids **11**, 2773 (1968).
6) A.F. Okuno and C. Park, J. Heat Transfer (Trans. ASME) **92**, 372 (1970).
7) D.D. Knight, AIAA J. **9**, 193 (1971).
8) M. Nishida, Phys. Fluids **15**, 596 (1972).
9) S.W. Bowen and C. Park, AIAA J. **9**, 493 (1971).
10) C. Park, J. Plasma Phys. **9**, 187 (1973).
11) D.D. McGregor and M. Mitchner, Phys. Fluids, **17**, 2155 (1974).
12) A. Kimura. K. Teshima and M. Nishida, Trans. Japan Soc. Aero. Space Sci. **18**, 103 (1975).
13) M. Nishida, Z. Naturforsch. **30a**, 1563 (1975).
14) M. Nishida, ZAMP **28**, 265 (1977).
15) Y. Takano, Doctoral Thesis, Kyoto University (1979).
16) A. Kimura and M. Nishida, Trans. Japan Soc. Aero. Space Sci. **27**, 162 (1979).
17) S.P. Knöös, J. Plasma Phys. **2**, 207 (1968).
18) C.H. Kruger and M. Mitchner, Phys. Fluids **10**, 1953 (1967).
19) G.W. Sutton and A. Sherman, Engineering Magnetohydrodynamics, McGraw-Hill, New York, Chapt. 4 (1965).
20) M.Y. Jaffrin, Phys. Fluids **8**, 606 (1965).

21) F.G. Blottner, AIAA J. **7**, 2281 (1961).
22) M.S. Grewal and L. Talbot, J. Fluid Mech. **16**, 573 (1963).
23) Y.M. Kagan, R.I. Lyagushchenko and A.D. Khakhaev, Optical Spectroscopy **15**, 5 (1963).
24) S. Byron, R.C. Stabler and P.I. Bortz, Phys. Rev. Letters **8**, 376 (1962).
25) M.J. Seaton, Atomic and Molecular Processes (Ed. D.R. Bates) Academic Press, New York, p. 374 (1962).
26) I.I. Sobelman, Introduction to the Theory of Atomic Spectra, Pergamon Press, Oxford, Chapt. 11 (1972).
27) H.W. Drawin, EUR-CEA-FC-383, Association Euratom-C.E.A., Fontenay-aux-Roses, France (1967).
28) K. Katsonis, EUR-CEA-FC-820, Association Euratom-C.E.A., Fontenay-aux-Roses, France (1976).
29) D.R. Bates and A. Damgaard, Phil. Trans. Roy. Soc. (London) **A242**, 101 (1950).

Appendix

Ambipolar Schmidt Number

The diffusion velocities of the electrons and ions are expressed respectively as,

$$\boldsymbol{V}_{d_e} = -\bar{\mu}_e \boldsymbol{E} - D_e \nabla p_e / p_e \,, \tag{A1}$$

$$\boldsymbol{V}_{d_i} = \bar{\mu}_i \boldsymbol{E} - D_i \nabla p_i / p_i \,, \tag{A2}$$

where $\bar{\mu}$ is the mobility, $\boldsymbol{E}$ the strength of electric field, D the diffusion coefficient, p the pressure, and subscripts e and i denote the electrons and ions, respectively. Multiplying Eq. (A1) by $\bar{\mu}_i$ and Eq. (A2) by $\bar{\mu}_e$, and summing the resultant equation, we have

$$\boldsymbol{V}_d = -\frac{\bar{\mu}_i + \bar{\mu}_e}{\bar{\mu}_i \bar{\mu}_e} D_e \frac{\nabla p_e}{p_e} - \frac{\bar{\mu}_e}{\bar{\mu}_i + \bar{\mu}_e} D_i \frac{\nabla p_i}{p_i} \,, \tag{A3}$$

where $\boldsymbol{V}_d = \boldsymbol{V}_{d_e} = \boldsymbol{V}_{d_i}$. In Eq. (A3), we have considered an ambipolar diffusion so that $\boldsymbol{V}_{d_e} = \boldsymbol{V}_{d_i}$. Using the Einstein relation $D/\mu = dkT/e$, we have

$$\boldsymbol{V}_d = -\frac{\bar{\mu}_i \bar{\mu}_e}{\bar{\mu}_i + \bar{\mu}_e} \frac{1}{e n_e} (\nabla p_e + \nabla p_i) \,. \tag{A4}$$

Since $p = n k_B T_a (1 + \alpha_e T_e / T_a)$,

$$p_e = \frac{p_e \cdot p}{p} = \frac{n_e k_B T_e \cdot p}{n k_B T_a (1 + \alpha_e T_e / T_a)} \,. \tag{A5}$$

Therefore we obtain

$$\nabla p_e = p \left[\frac{\Omega}{(1 + \alpha_e \Omega)^2} \nabla \alpha_e + \frac{\alpha_e}{(1 + \alpha_e \Omega)^2} \nabla \Omega \right] + \frac{\alpha_e \Omega}{1 + \alpha_e \Omega} \nabla p \,, \tag{A6}$$

Similarly,

$$\nabla p_i = \nabla\left[\frac{n_e k_B T_a \cdot p}{n k_B T_a (1+\alpha_e T_e/T_a)}\right]$$
$$= p\left[\frac{1}{(1+\alpha_e\Omega)^2}\nabla\alpha_e - \frac{\alpha_e^2}{(1+\alpha_e\Omega)^2}\nabla\Omega\right] + \frac{\alpha_e}{1+\alpha_e\Omega}\nabla p\,. \tag{A7}$$

Using Eqs. (A6) and (A1),

$$V_d = -\frac{\bar{\mu}_i\bar{\mu}_e}{\bar{\mu}_i+\bar{\mu}_e}\frac{kT_a}{e}\left[\frac{1+\Omega}{1+\alpha_e\Omega}\nabla\alpha + \frac{\alpha_e(1-\alpha_e)}{1+\alpha_e\Omega}\nabla\Omega + \alpha_e(1+\alpha_e)\frac{\nabla p}{p}\right]$$
$$= -\frac{\bar{\mu}_i\bar{\mu}_e}{\bar{\mu}_i+\bar{\mu}_e}\frac{kT_a}{e}\frac{1+\Omega}{1+\alpha_e\Omega}\left[\frac{\nabla\alpha_e}{\alpha_e} + \frac{1-\alpha_e}{1+\Omega}\nabla\Omega + (1+\alpha_e\Omega)\frac{\nabla p}{p}\right]. \tag{A8}$$

The ambipolar diffusion coefficient D_a is defined as

$$D_a = \frac{\bar{\mu}_e\bar{\mu}_i}{\bar{\mu}_e+\bar{\mu}_i}\frac{k_B T_a}{e}\frac{1+\Omega}{1+\alpha_e\Omega}\,. \tag{A9}$$

Since p=const near the stagnation point in the shock layer, the third term in the bracket vanishes. Eq. (A8) is rewritten as

$$V_d = -D_a\left[\frac{\nabla\alpha_e}{\alpha_e} + \frac{1-\alpha_e}{1+\Omega}\nabla\Omega\right]. \tag{A10}$$

Using the relations $\bar{\mu}_e \gg \bar{\mu}_i$ and $\bar{\mu}_i \simeq e/m_i\bar{\nu}_{ia}$, D_a is expressed as

$$D_a \simeq \frac{k_B T_a}{m_a \nu_{ia}}\frac{1+\Omega}{1+\alpha_e\Omega}\,. \tag{A11}$$

In the practical calculations, the ambipolar Schmidt number $Sc_a=\mu/\rho D_a$ is often employed rather than the ambipolar diffusion coefficient D_a. If the degree of ionization is negligible compared with unity, the viscosity μ is expressed as

$$\mu = \frac{5\pi}{32}\frac{m_a}{\sigma_{aa}}\left(\frac{8kT_a}{\pi m_a}\right)^{1/2}, \tag{A12}$$

where σ_{aa} is the collision cross section for atom-atom encounters. Substituting Eqs. (A11) and (A12) into the expression of the ambipolar Schmidt number, we have

$$Sc_a = \frac{5}{4}\frac{\sigma_{ia}(1-\alpha_e)(1+\alpha_e\Omega)}{\sigma_{aa}(1+\Omega)} = \frac{5}{4}\frac{\sigma_{ia}}{\sigma_{aa}}\frac{(1-\alpha_e)(T_a+\alpha_e T_e)}{T_a+T_e}\,. \tag{A13}$$

Erratum : Nonequilibrium Blunt Body Flows in Ionized Gases

Michio NISHIDA

Department of Aeronautical Engineering

Page 273 : The second term on the L.H.S. of Eq. (30) and the second term on the L.H.S. of Eq. (31) are misprinted. The correct terms are, for Eq. (30)

$$\frac{d}{d\eta}\left[\frac{\ell}{Sc_a}\frac{\tau(1-\alpha_{e_s}z)z}{1+\tau\bar{\Omega}}\frac{d\bar{\Omega}}{d\eta}\right] ,$$

and for Eq. (31)

$$\alpha_{e_s}\frac{d}{d\eta}\left[\theta\left\{\frac{\ell}{Sc_a}\frac{dz}{d\eta}+\frac{\ell}{Sc_a}\frac{\tau(1-\alpha_{e_s}z)z}{1+\tau\bar{\Omega}}\frac{d\bar{\Omega}}{d\eta}\right\}\right] .$$